Electronic Supplementary Material (ESI) for Inorganic Chemistry Frontiers.
This journal is © the Partner Organisations 2024

Supporting Information

Interface synergetic enhanced $Co_2P/CoMoP_2$ heterojunction electrocatalytic performance for hydrogen production from water/seawater splitting

Bo Sun [1], Chunhu Li [1], Jie Yang[1], Hongcun Bai[2] and Xiangchao Meng[1*]*

[1]Key Laboratory of Marine Chemistry Theory and Technology (Ministry of Education), College of Chemistry & Chemical Engineering, Ocean University of China, Qingdao, Shandong, 266100, China.

[2]State Key Laboratory of High-efficiency Utilization of Coal and Green Chemical Engineering, Ningxia University, Yinchuan, Ningxia 750021, China.

[*]Corresponding authors.

Emails: lichunhu@ouc.edu.cn (C. L.); mengxiangchao@ouc.edu.cn (X. M.)

S1. Synthesis of comparsion samples

S1.1 Synthesis of Co_2P nanobricks array on NF

To synthesize Co_2P, Co-BDC/NF and NaH_2PO_2 (1 g) were placed on opposite sides of a porcelain boat. The subsequent reaction process followed the same steps as that of $Co_2P/CoMoP_2$ (referred to as Co_2P).

S1.2 Synthesis of $CoMoP_2$ nanosheets array on NF

Firstly, for the synthesis of $CoMoO_4$ nanosheets, 1.8 mmol of $Co(NO)_3 \cdot 6H_2O$ and 1.8 mmol of $Na_2MoO_4 \cdot 2H_2O$ were dissolved in 30 ml of water to create a transparent solution. The subsequent reaction process followed the same steps as that of Co-BDC/NF, denoted as $CoMoO_4$/NF. Subsequently, the resulting $CoMoO_4$/NF and 1 g of NaH_2PO_2 were positioned on opposite sides of a porcelain boat. The subsequent reaction process mirrored that of $Co_2P/CoMoP_2$, denoted as $CoMoP_2$.

S1.3 Synthesis electrode of Pt/C and RuO_2 on NF

To synthesize the Pt/C electrode on NF, a solution was formed by dissolving 5 mg of commercial Pt/C (20 wt%) and 40 μL of Nafion solution in 1 ml of ethanol, followed by 30 minutes of sonication to achieve a uniform ink. This ink was then applied to a clean NF, covering an area of 1 cm^2 with approximately 5 mg of the electrode material. The electrode was left to dry at room temperature overnight, resulting in the formation

of NF-supported Pt/C. The synthesis of the RuO_2 electrode followed the same procedure as that of the Pt/C electrode, with a loading of 5 mg cm^{-2}.

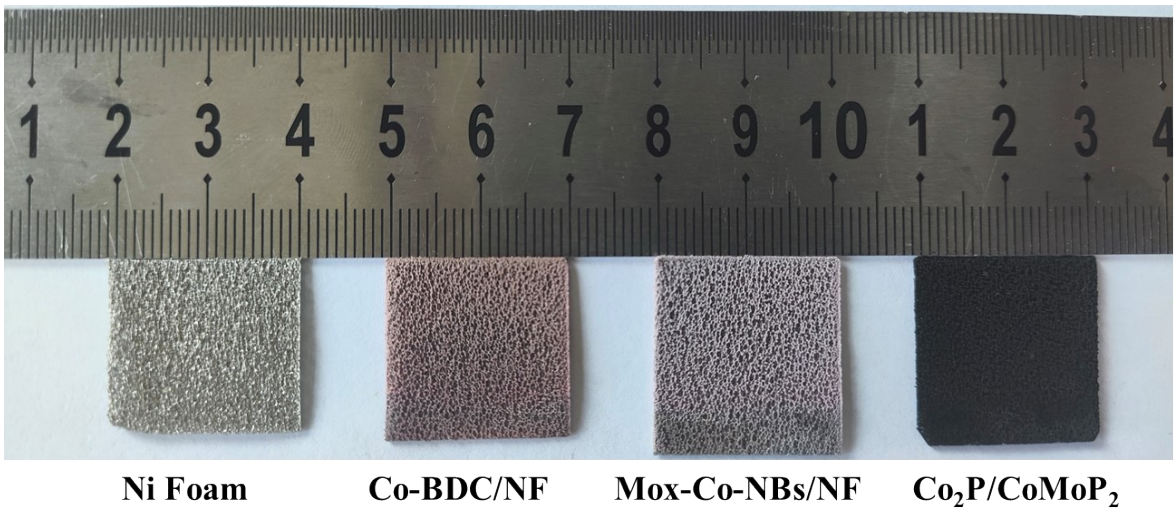

Figure S1. *The optical photographs of samples.*

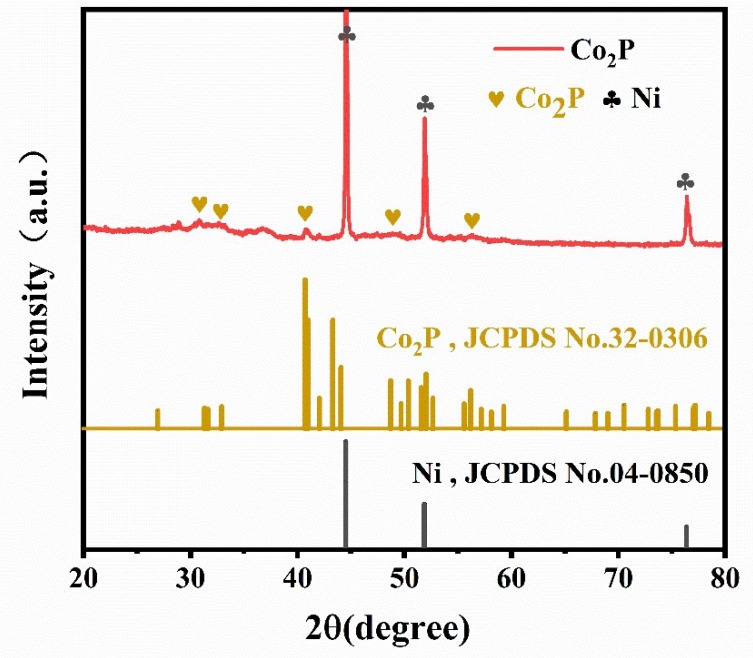

Figure S2. *The XRD pattern of Co_2P /NF.*

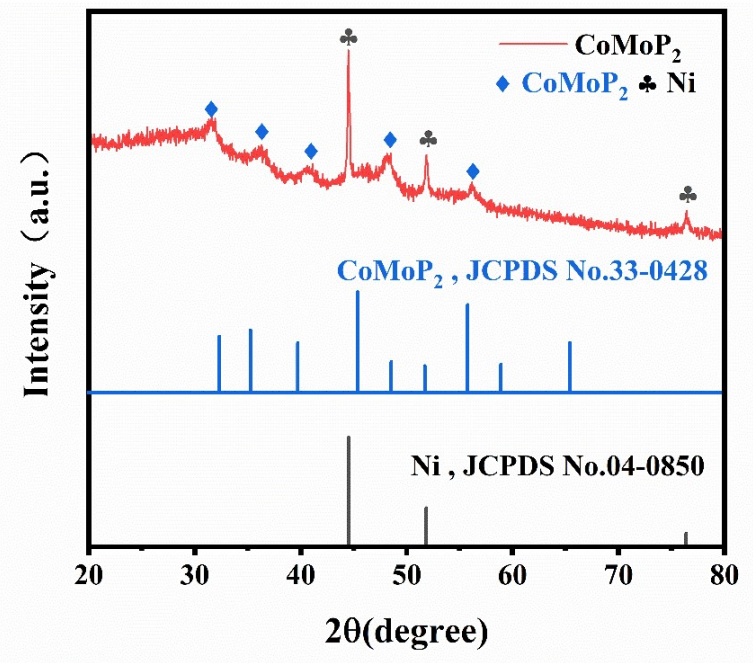

Figure S3. *The XRD pattern of* $CoMoP_2$ */NF.*

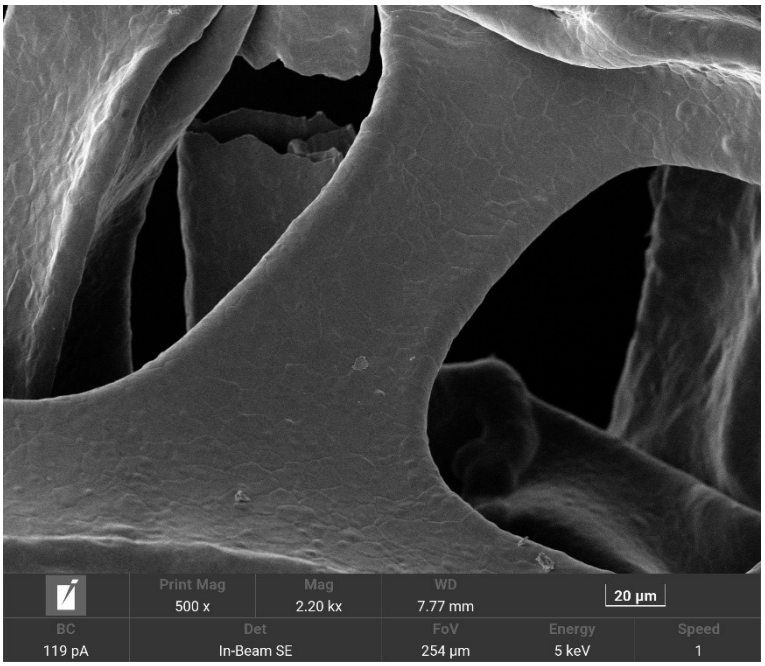

Figure S4. *SEM image of Ni foam.*

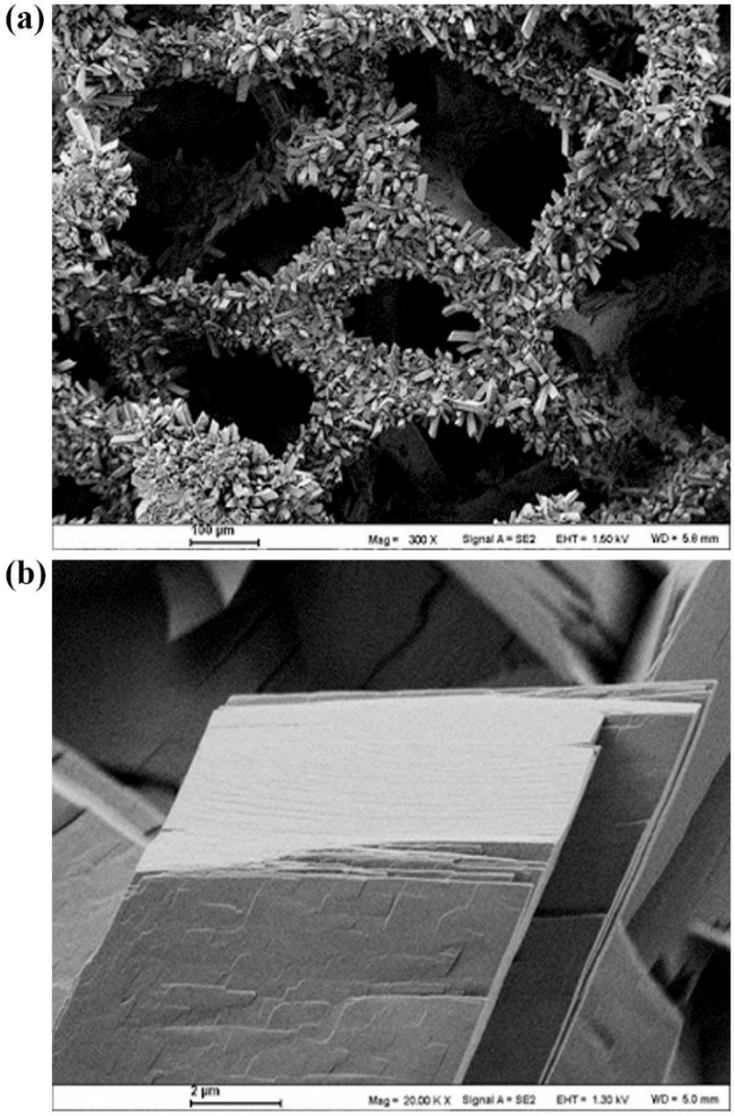

Figure S5. *(a) SEM image and (b) high-resolution SEM image of Co-BDC/NF.*

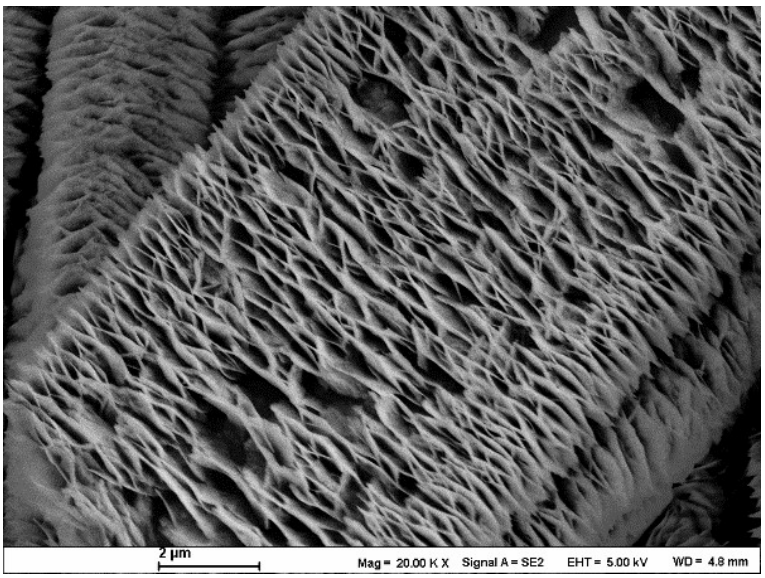

Figure S6. *High-resolution SEM image of Mo-Co-NBs/NF.*

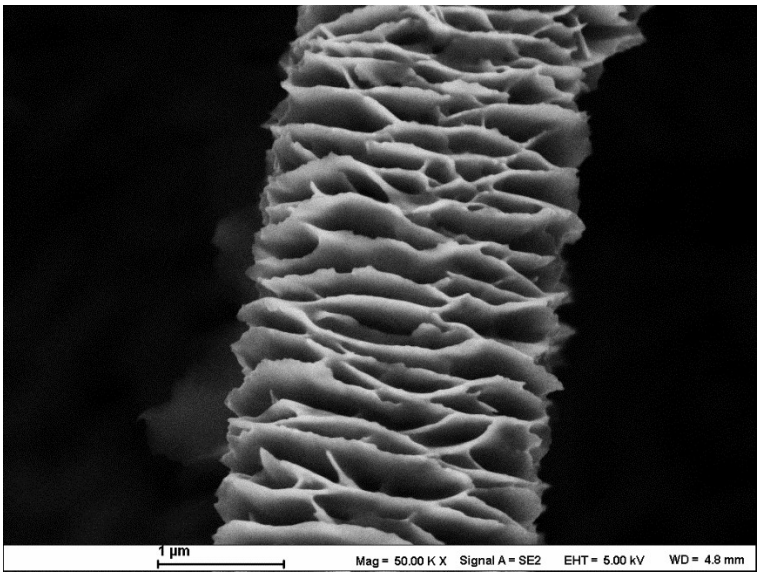

Figure S7. *High-resolution SEM image of $Co_2P/CoMoP_2$.*

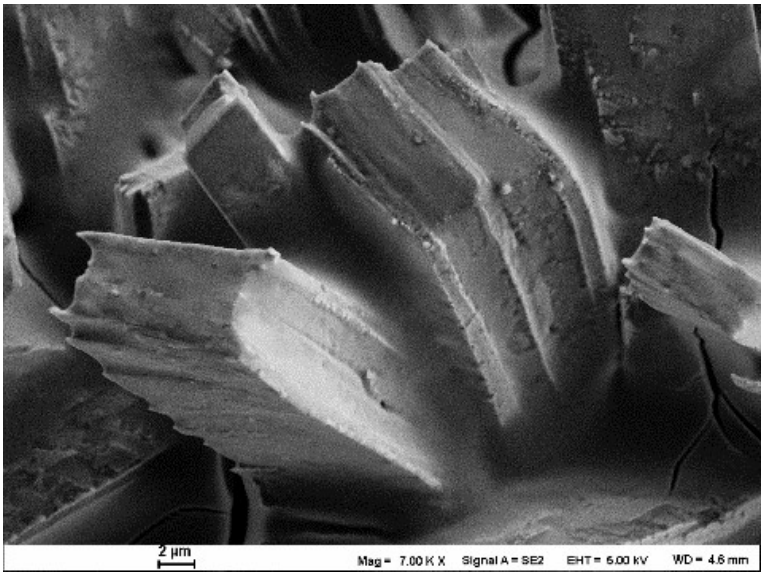

Figure S8. *High-resolution SEM image of Co_2P /NF.*

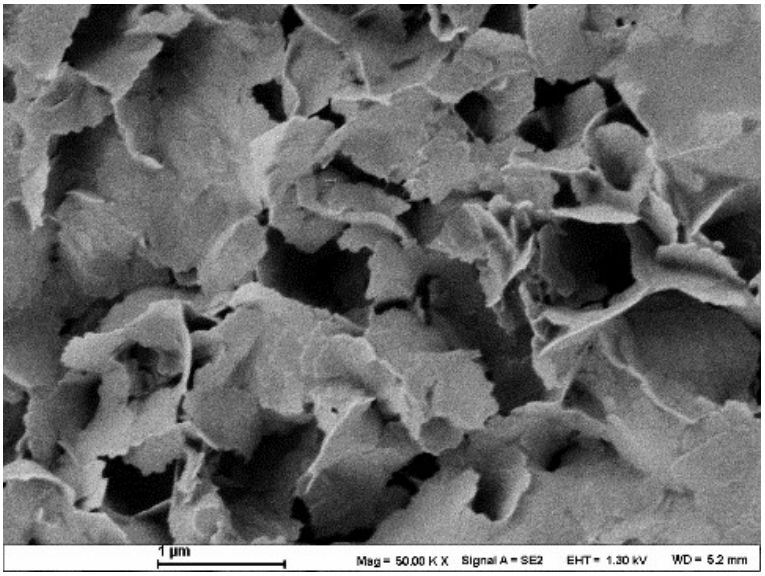

Figure S9. *High-resolution SEM image of* $CoMoP_2$ */NF.*

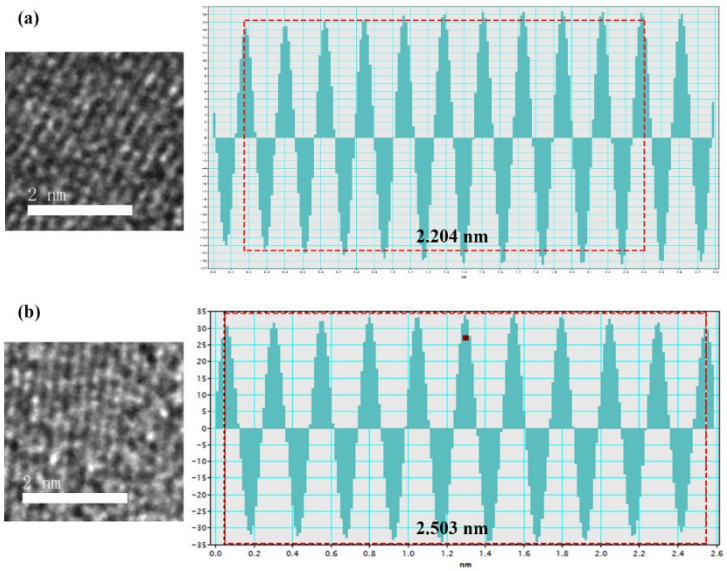

Figure S10. *Interplanar spacing of Co_2P (121) and $CoMoP_2$ (102), respectively.*

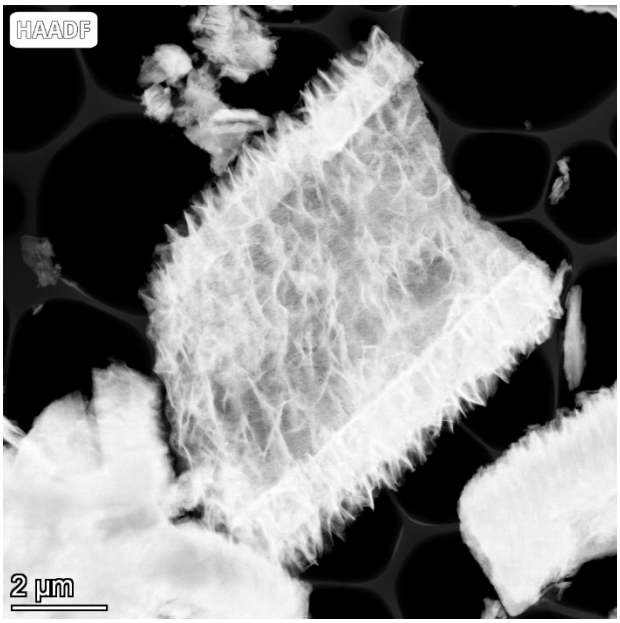

Figure S11. *High-angle annular dark-field(HAADF)-TEM image of Co_2P / $CoMoP_2$.*

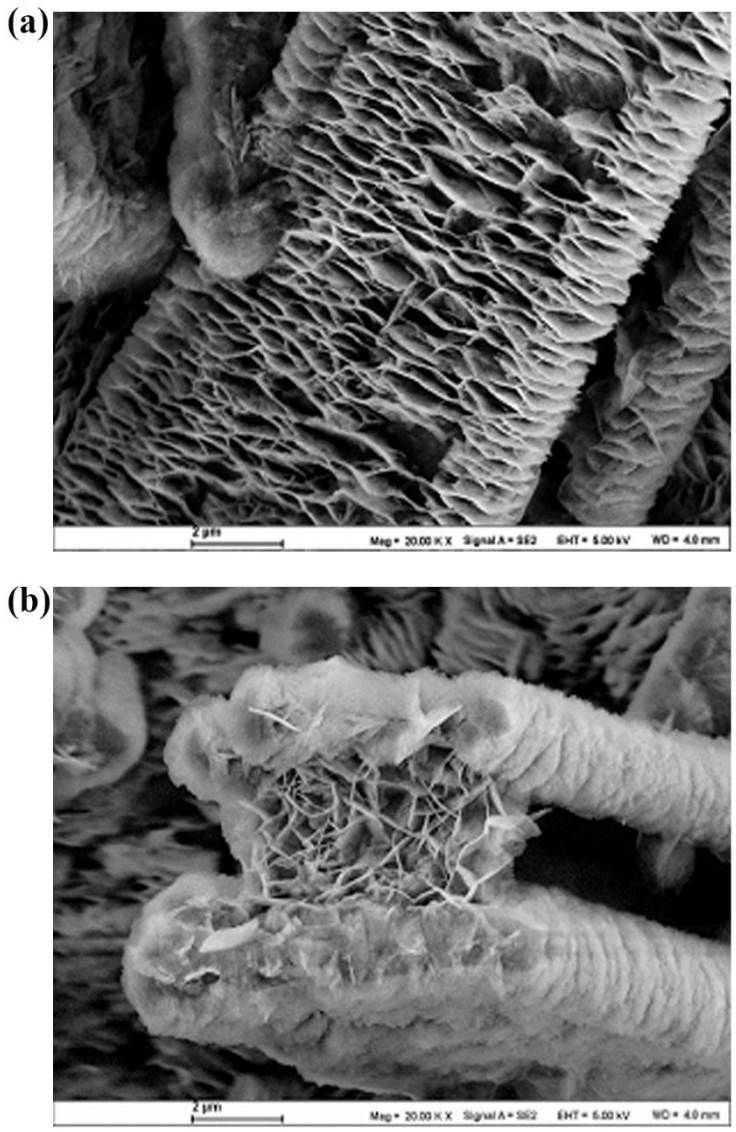

Figure S12. *SEM images of $Co_2P/CoMoP_2$ after durability HER test in (a) alkaline and (b) alkaline seawater solution.*

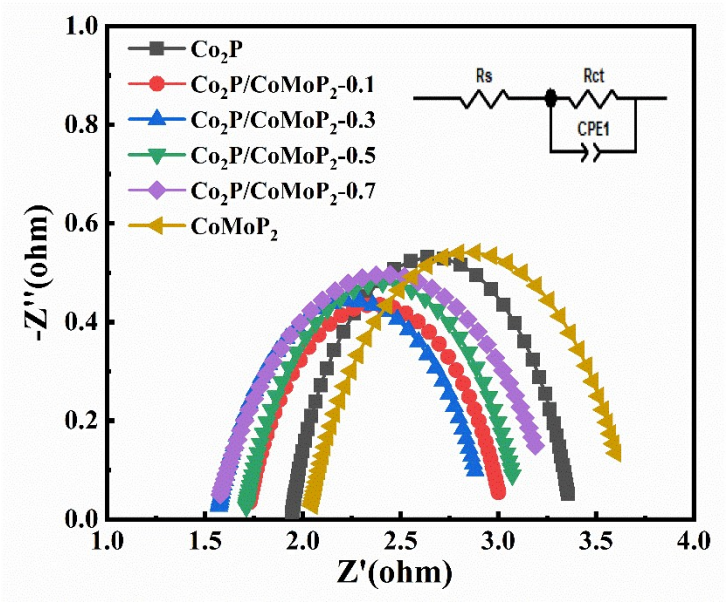

Figure S13. *Nyquist plots of various catalysts at 10 mA cm^{-2}.*

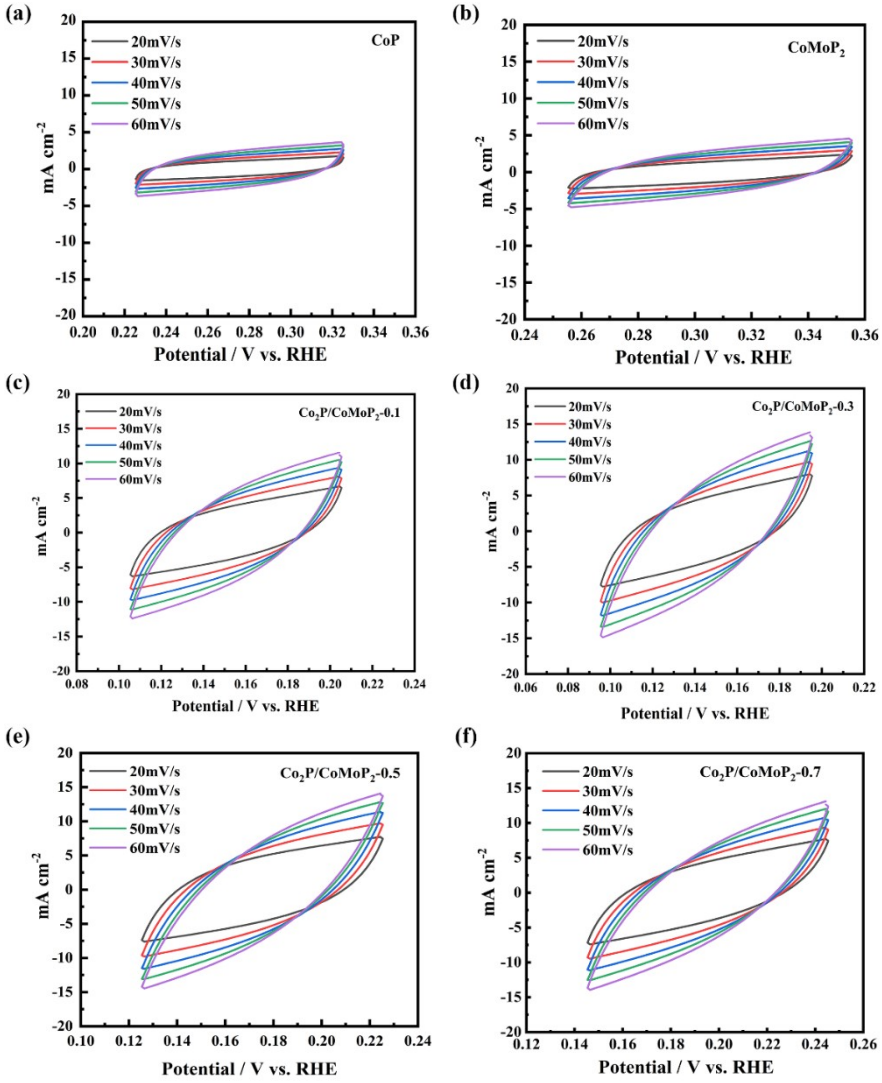

Figure S14. *Cyclic voltammograms (CV) curves of (a) Co_2P, (b) $CoMoP_2$, (c) $Co_2P/CoMoP_2$-0.1, (d) $Co_2P/CoMoP_2$-0.3, (e) $Co_2P/CoMoP_2$-0.5 and (f) $Co_2P/CoMoP_2$-0.7.*

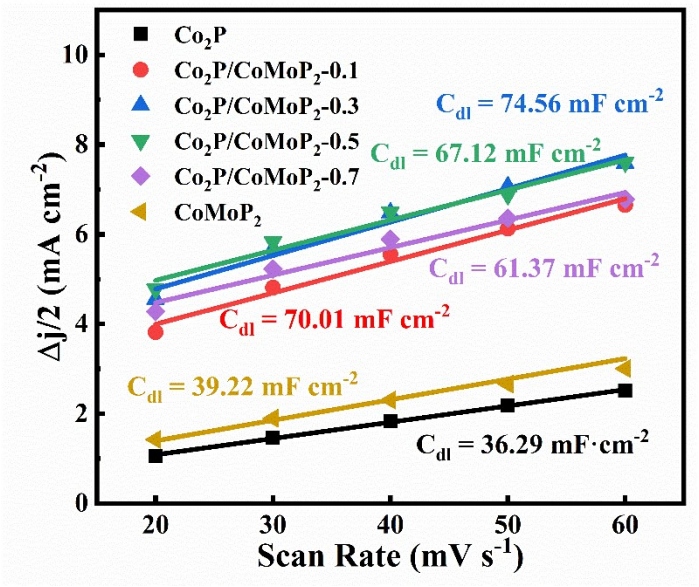

Figure S15. *The C_{dl} values of various catalysts.*

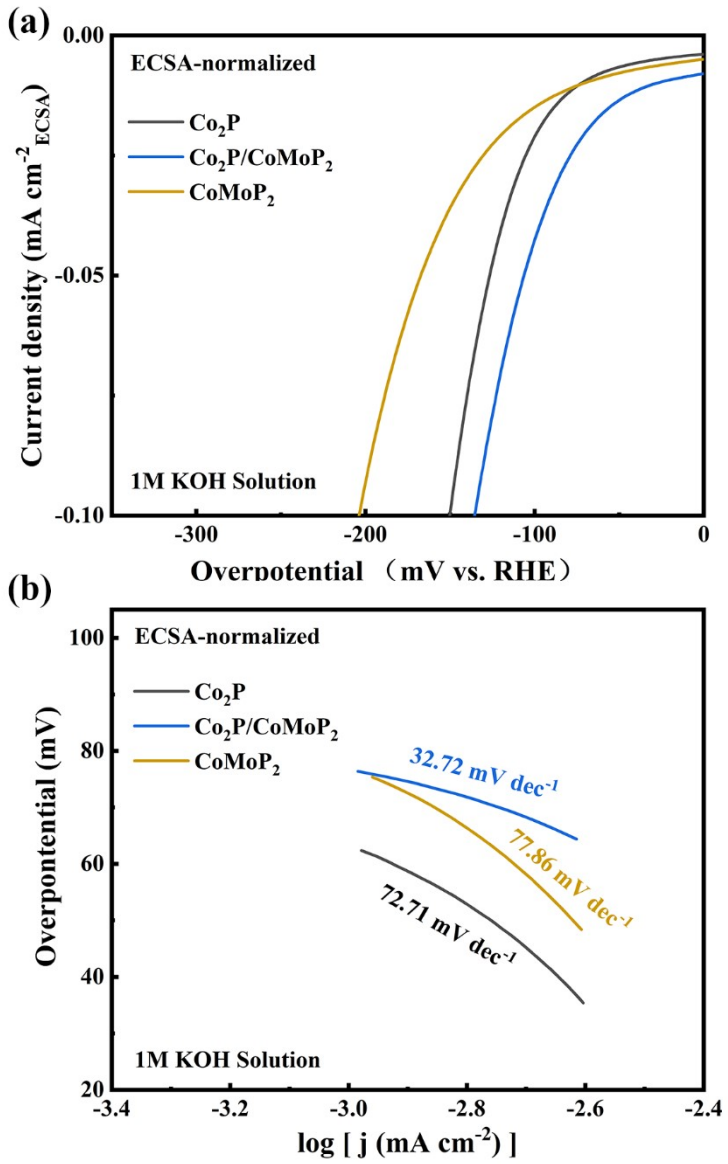

Figure S16. *The ESCA-normalized of HER test (a) polarization curves and (b) corresponding Tafel plots of $Co_2P/CoMoP_2$, Co_2P and $CoMoP_2$ in 1 M KOH solution.*

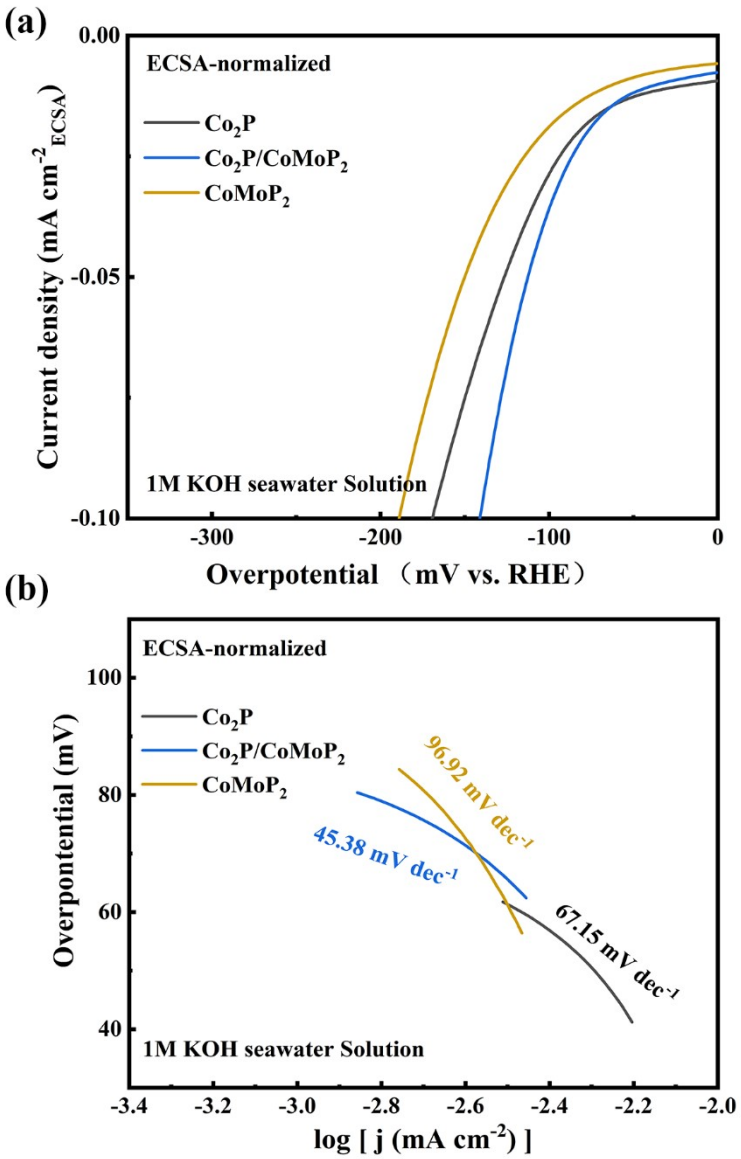

Figure S17. *The ESCA-normalized of HER test (a) polarization curves and (b) corresponding Tafel plots of $Co_2P/CoMoP_2$, Co_2P and $CoMoP_2$ in 1 M KOH seawater solution.*

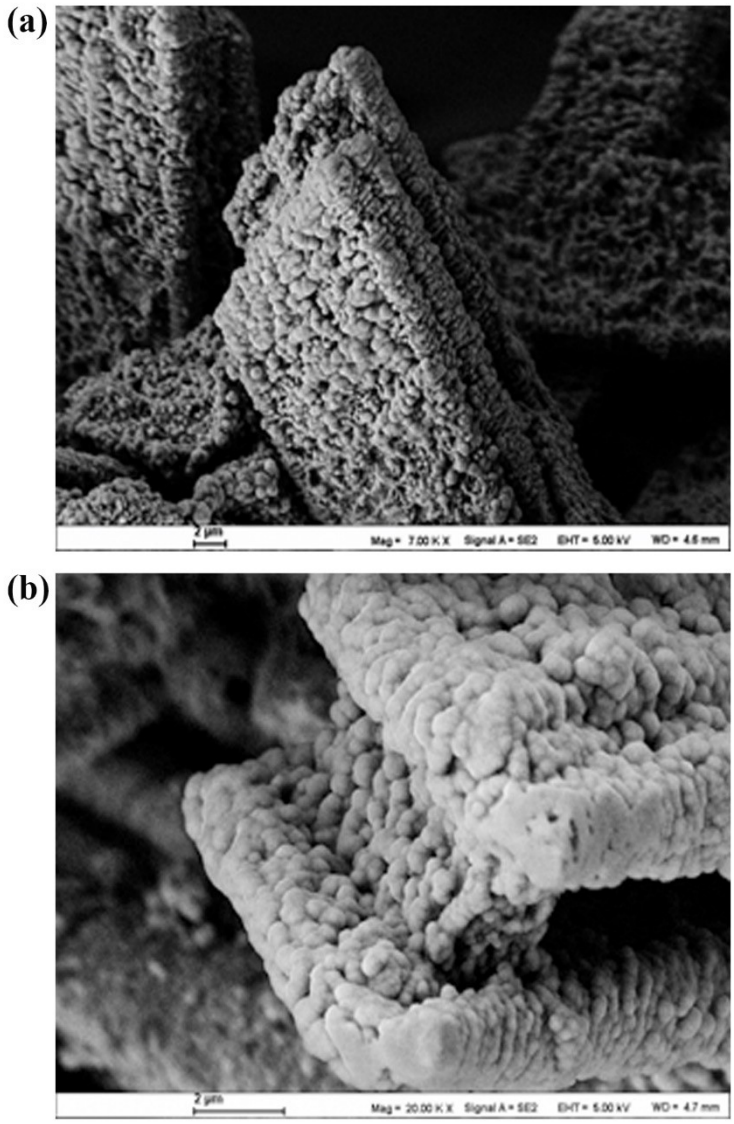

Figure S18. *SEM images of $Co_2P/CoMoP_2$ after durability OER test in (a) alkaline and (b) alkaline seawater solution.*

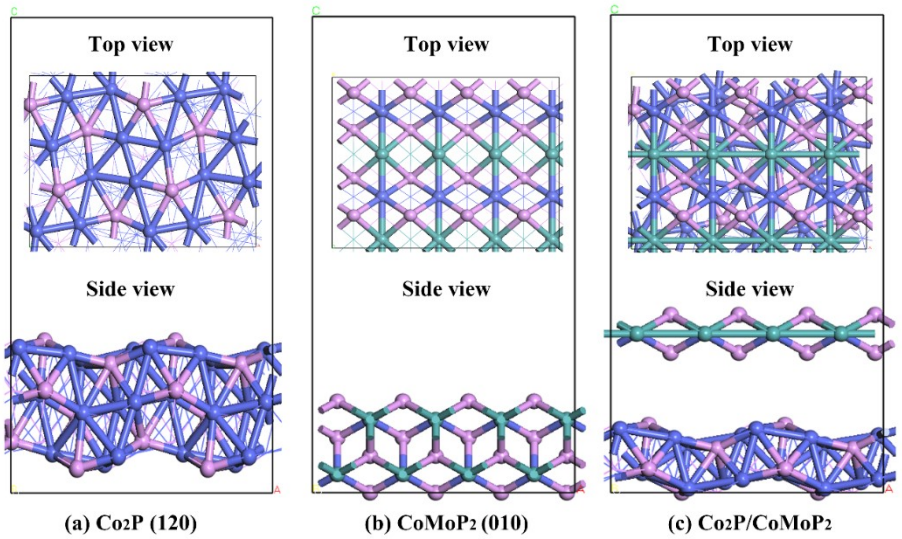

Figure S19. *The schematic of calculation models of (a) Co_2P, (b) $CoMoP_2$ and (c) Co_2P/ $CoMoP_2$, respectively. (P atoms: pink balls, Co atoms: blue balls and Mo atoms: green balls).*

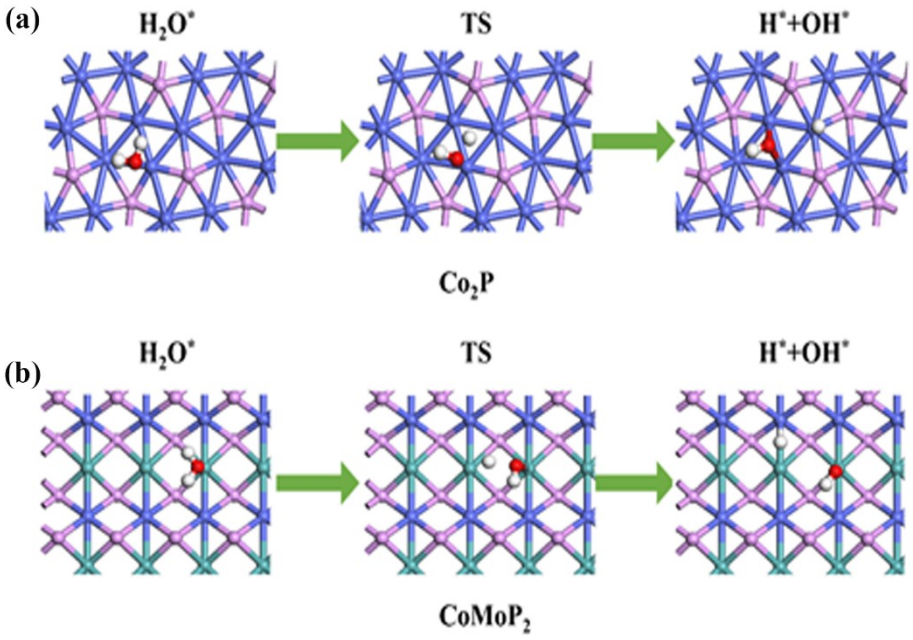

Figure S20. *The top views of schematic models of water dissociation on CoP_2 (a) and $CoMoP_2$ (b) surface. The white, red, pink, blue and green balls represent the H, O, P, Co and Mo atoms, respectively.*

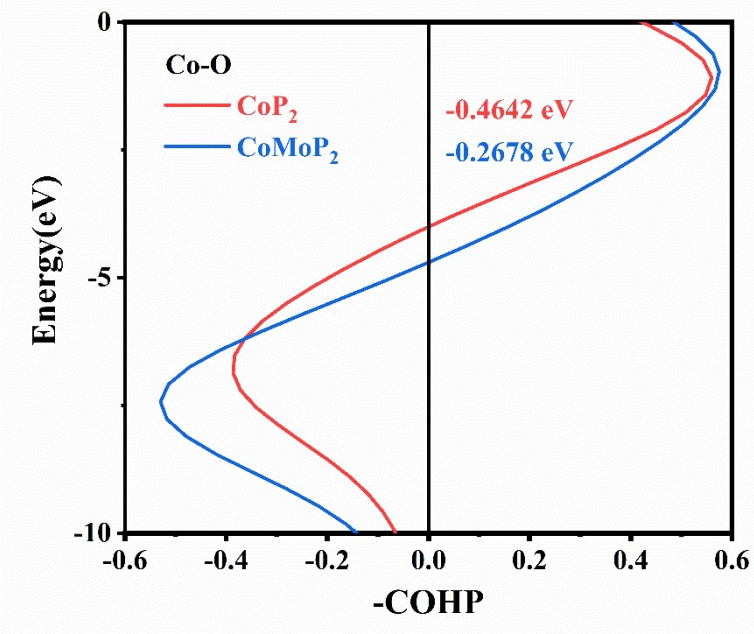

Figure S21. *The bonding strength of Co-O after H_2O activation on the surface of Co_2P and $CoMoP_2$, respectively.*

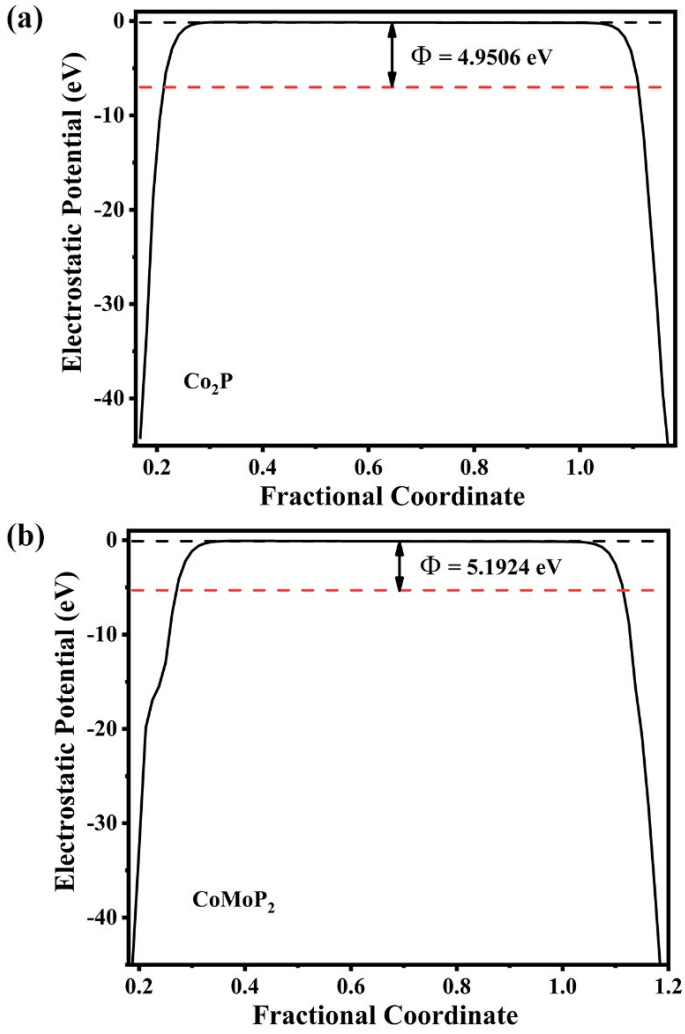

Figure S22. *Work function of (a) Co_2P and (b) $CoMoP_2$, respectively.*

Table S1. HER performances of $Co_2P/CoMoP_2$ and other reported electrocatalysts in alkaline media. (1 M KOH)

Catalyst	Substrate	η_{10} (j=10 mA cm^{-2})	Tafel slope (mV dec^{-1})	Ref.
$Co_2P/CoMoP_2$	NF	36	57.74	This work
Co_2P/BNP-CNTs	GCE	133	90	[1]
CuO@Co_2P	CF	150	56.66	[2]
N–$Co_2P/NiCo_2O_4$	NF	58	75	[3]
CoxP/Cu-Co_9S_8	NF	118	66.75	[4]
CoP3/CoMoP	NF	110	64.1	[5]
Co-Mo-Ni-P	CF	106@100 mA cm^{-2}	62.57	[6]
Co(II)Mo(IV)P	NF	39	73.3	[7]
$MoS_2/CoMoP_2$	NA	75	NA	[8]
La-CoMoP	GCE	49	88.9	[9]
CoMo/CoMoP	NF	61	46.4	[10]
N−Co_2P	CC	34	51	[11]
$Co_2P/CoWO_4$	NF	81	47	[12]
Co_2P@3D-rGO	NF	36.5	55.5	[13]
Co_2P @ C	GCE	157	93.8	[14]

NF: Ni foam; GCE: glassy carbon rotating electrode; CF: Cu foam; CC: Carbon Cloth; SS: Stainless Steel.

Table S2. HER performances of $Co_2P/CoMoP_2$ and other reported electrocatalysts in alkaline seawater media. (1 M KOH seawater)

Catalyst	Substrate	η_{10} (j=10 mA cm^{-2})	Tafel slope (mV dec^{-1})	Ref.
$Co_2P/CoMoP_2$	NF	43	58	This work
Ni-WO_x	NF	45.69	46	[15]
CoP_x	NF	117	71.1	[16]
Ni-SA/NC	-	139	123	[17]
$Cu_{0.98}La_{0.02}O$	SS	170	181	[18]
Fe,P-$NiSe_2$		182	48.9	[19]
2Dmeso-Mo_2C/Mo_2N	-	197	67.6	[20]

Table S3. R_s and R_{ct} of all the as-obtained catalysts.

Samples	R_s **(Ω)**	R_{ct} **(Ω)**
Co_2P	1.94	1.48
$CoMoP_2$	2.00	1.72
$Co_2P/CoMoP_2$-0.1	1.71	1.31
$Co_2P/CoMoP_2$-0.3	1.56	1.37
$Co_2P/CoMoP_2$-0.5	1.70	1.41
$Co_2P/CoMoP_2$-0.7	1.54	1.74

Table S4. ECSA surface area of all the as-obtained catalysts.

Samples	C_{dl} (mF)	ECSA (m^2)
Co_2P	36.29	0.0907
$CoMoP_2$	39.22	0.0980
$Co_2P/CoMoP_2$-0.1	70.01	0.1750
$Co_2P/CoMoP_2$-0.3	74.56	0.1864
$Co_2P/CoMoP_2$-0.5	67.12	0.1678
$Co_2P/CoMoP_2$-0.7	61.37	0.1534

Table S5. OER performances of $Co_2P/CoMoP_2$ and other reported electrocatalysts in 1 M KOH and 1 M KOH seawater solution.

Catalyst	Electrolyte	η_{10} (j=10 mA cm^{-2})	Tafel slope (mV dec^{-1})	Ref.
$Co_2P/CoMoP_2$	1 M KOH	254	61.24	This work
	1 M KOH seawater	268	81.00	
Co-Ru@RuO_x/NCN	1 M KOH	270	67	[21]
$Zn^{0.1}$-CoP	1 M KOH	290	56	[22]
FeCoP	1 M KOH	340	60.7	[23]
MoS_2/CoFe@NC	1 M KOH	337	84.6	[24]
Co-Ni_3S_2/NF	1 M KOH	368@100 mA cm^{-2}	50	[25]
0.5Fe-$NiCo_2O_4$@CC	1 M KOH	258	63.5	[26]
	1 M KOH seawater	273	76.1	
Cr-Co_XP	1 M KOH seawater	334@ 100 mA cm^{-2}	-	[27]
Co–CoO@C	1 M KOH seawater	374	70.07	[28]

Table S6. Comparison of catalytic performance for alkaline water/seawater electrolysis

Cathode	Anode	Electrolyte	Cell voltage(V) at 10 mA cm^{-2}	Cell voltage(V) at 50 mA cm^{-2}	Ref.
$Co_2P/CoMoP_2$	$Co_2P/CoMoP_2$	1 M KOH	1.59	1.68	This work
		1 M KOH seawater	1.61	1.72	This work
CoP Nanoframes	CoP Nanoframes	1 M KOH	1.65	NA	[29]
CoFeZr oxides	CoFeZr oxides	1 M KOH	1.63	NA	[30]
Co/β-Mo_2C@NCNTs	Co/β-Mo_2C@NCNTs	1 M KOH	1.64	NA	[31]
CoP-PBSCF	CoP-PBSCF	1 M KOH	1.69	NA	[32]
$Co_2Mo_3O_8/MoO_2$	$Co_2Mo_3O_8/MoO_2$	1 M KOH	NA	1.69	[33]
$MoNi_4/MoO_x$	$MoNi_4/MoO_x$	1 M KOH	NA	1.67	[34]
La-CoMoP	La-CoMoP	1 M KOH	1.56	NA	[9]
CoMo/CoMoP	CoMo/CoMoP	1 M KOH	1.54	NA	[10]
$NiSe_2$@Fe–NiCo LDH	$NiSe_2$@Fe–NiCo LDH	1 M KOH	1.64	NA	[35]
Co_3S_4/Co_3O_4	Co_3S_4/Co_3O_4	1 M KOH	1.59	NA	[36]
		1 M KOH seawater	1.67	NA	
NiCoN|NixP|Ni CoN	NiCoN|NixP|Ni CoN	1 M KOH seawater	1.81	NA	[37]
$Co_2P/NiWO_4$	$Co_2P/NiWO_4$	1 M KOH seawater	1.59	NA	[38]

References

[1] A. Ali, Y. Liu, R. Mo, P. Chen, P.K. Shen, Facile one-step in-situ encapsulation of non-noble metal Co_2P nanoparticles embedded into B, N, P tri-doped carbon nanotubes for efficient hydrogen evolution reaction, International Journal of Hydrogen Energy 45(46) (2020) 24312-24321. https://doi.org/10.1016/j.ijhydene.2020.06.235.

[2] M. Bi, Z. Guo, Z. Liu, M. Ruan, Efficient and stable electrocatalytic performances of nanostructured composite of CuO and Co_2P in the full pH range towards hydrogen and oxygen evolution, Colloids and Surfaces A: Physicochemical and Engineering Aspects 673 (2023). https://doi.org/10.1016/j.colsurfa.2023.131802.

[3] X. Ji, X. Chen, L. Zhang, C. Meng, Y. He, X. Zhang, Z. Wang, R. Yu, Anchoring nitrogen-doped Co_2P nanoflakes on $NiCo_2O_4$ nanorod arrays over nickel foam as high-performance 3D electrode for alkaline hydrogen evolution, Green Energy & Environment 8(2) (2023) 470-477. https://doi.org/10.1016/j.gee.2021.05.010.

[4] D. Jiang, W. Ma, Y. Zhou, Y. Xing, B. Quan, D. Li, Coupling Co(2)P and CoP nanoparticles with copper ions incorporated Co(9)S(8) nanowire arrays for synergistically boosting hydrogen evolution reaction electrocatalysis, J Colloid Interface Sci 550 (2019) 10-16. https://doi.org/10.1016/j.jcis.2019.04.080.

[5] D. Jiang, Y. Xu, R. Yang, D. Li, S. Meng, M. Chen, CoP_3/CoMoP Heterogeneous Nanosheet Arrays as Robust Electrocatalyst for pH-Universal Hydrogen Evolution Reaction, ACS Sustainable Chemistry & Engineering 7(10) (2019) 9309-9317.

https://doi.org/10.1021/acssuschemeng.9b00357.

[6] J. Jin, F. Chen, Y. Feng, J. Zhou, W. Lei, F. Gao, Co-Ni-Mo phosphides hierarchical nanoarrays as bifunctional electrocatalysts for excellent overall water splitting, Fuel 332 (2023). https://doi.org/10.1016/j.fuel.2022.126131.

[7] D. Li, D. Liu, S. Zhao, S. Lu, Y. Ma, M. Li, G. Chen, Y. Wang, G. Zhou, C. Xiao, Tuning of metallic valence in CoMoP for promoting electrocatalytic hydrogen evolution, International Journal of Hydrogen Energy 44(59) (2019) 31072-31081. https://doi.org/10.1016/j.ijhydene.2019.10.016.

[8] G. Li, C. Fu, J. Wu, J. Rao, S.-C. Liou, X. Xu, B. Shao, K. Liu, E. Liu, N. Kumar, X. Liu, M. Fahlman, J. Gooth, G. Auffermann, Y. Sun, C. Felser, B. Zhang, Synergistically creating sulfur vacancies in semimetal-supported amorphous MoS_2 for efficient hydrogen evolution, Applied Catalysis B: Environmental 254 (2019) 1-6. https://doi.org/10.1016/j.apcatb.2019.04.080.

[9] L. Li, K. Chao, X. Liu, S. Zhou, Construction of La decorated CoMoP composite and its highly efficient electrocatalytic activity for overall water splitting in alkaline media, Journal of Alloys and Compounds 941 (2023). https://doi.org/10.1016/j.jallcom.2023.168952.

[10] Y. Lu, X. Zheng, Y. Liu, J. Zhu, D. Li, D. Jiang, Synergistically Coupled CoMo/CoMoP Electrocatalyst for Highly Efficient and Stable Overall Water Splitting, Inorg Chem 61(21) (2022) 8328-8338. https://doi.org/10.1021/acs.inorgchem.2c00923.

[11] Y. Men, P. Li, J. Zhou, G. Cheng, S. Chen, W. Luo, Tailoring the Electronic

Structure of Co_2P by N Doping for Boosting Hydrogen Evolution Reaction at All pH Values, ACS Catalysis 9(4) (2019) 3744-3752. https://doi.org/10.1021/acscatal.9b00407.

[12] K. Tao, H. Dan, Y. Hai, L. Liu, Y. Gong, Ultrafine Co_2P anchored on porous $CoWO_4$ nanofiber matrix for hydrogen evolution: Anion-induced compositional/morphological transformation and interfacial electron transfer, Electrochimica Acta 328 (2019). https://doi.org/10.1016/j.electacta.2019.135123.

[13] Y. Wang, T. Wang, M. Yang, Y. Rui, Z. Xue, H. Zhu, C. Wang, J. Li, B. Chen, Co(2)P nanowire arrays anchored on a 3D porous reduced graphene oxide matrix embedded in nickel foam for a high-efficiency hydrogen evolution reaction, Dalton Trans 52(33) (2023) 11526-11534. https://doi.org/10.1039/d3dt01367g.

[14] Y. Wei, Q. Tian, L. Ji, T. Wang, S. Wang, Phytic acid-assisted fabrication of porous leaf-like hollow structured Co_2P @ C for efficient hydrogen evolution, Journal of Alloys and Compounds 934 (2023). https://doi.org/10.1016/j.jallcom.2022.167924.

[15] W. Liang, M. Zhou, X. Lin, J. Xu, P. Dong, Z. Le, M. Yang, J. Chen, F. Xie, N. Wang, Y. Jin, H. Meng, Nickel-doped tungsten oxide promotes stable and efficient hydrogen evolution in seawater, Applied Catalysis B: Environmental 325 (2023). https://doi.org/10.1016/j.apcatb.2023.122397.

[16] L. Wu, L. Yu, B. McElhenny, X. Xing, D. Luo, F. Zhang, J. Bao, S. Chen, Z. Ren, Rational design of core-shell-structured CoP @FeOOH for efficient seawater electrolysis, Applied Catalysis B: Environmental 294 (2021).

https://doi.org/10.1016/j.apcatb.2021.120256.

[17] W. Zang, T. Sun, T. Yang, S. Xi, M. Waqar, Z. Kou, Z. Lyu, Y.P. Feng, J. Wang, S.J. Pennycook, Efficient Hydrogen Evolution of Oxidized Ni-N(3) Defective Sites for Alkaline Freshwater and Seawater Electrolysis, Adv Mater 33(8) (2021) e2003846. https://doi.org/10.1002/adma.202003846.

[18] J.D. Rodney, S. Deepapriya, M.C. Robinson, S.J. Das, S. Perumal, P. Sivakumar, H. Jung, B.C. Kim, C.J. Raj, Cu1-xRExO (RE = La, Dy) decorated dendritic CuS nanoarrays for highly efficient splitting of seawater into hydrogen and oxygen fuels, Applied Materials Today 24 (2021). https://doi.org/10.1016/j.apmt.2021.101079.

[19] J. Chang, G. Wang, Z. Yang, B. Li, Q. Wang, R. Kuliiev, N. Orlovskaya, M. Gu, Y. Du, G. Wang, Y. Yang, Dual-Doping and Synergism toward High-Performance Seawater Electrolysis, Adv Mater 33(33) (2021) e2101425. https://doi.org/10.1002/adma.202101425.

[20] S. Li, Z. Zhao, T. Ma, P. Pachfule, A. Thomas, Superstructures of Organic-Polyoxometalate Co-crystals as Precursors for Hydrogen Evolution Electrocatalysts, Angew Chem Int Ed Engl 61(3) (2022) e202112298. https://doi.org/10.1002/anie.202112298.

[21] H. Wang, P. Yang, X. Sun, W. Xiao, X. Wang, M. Tian, G. Xu, Z. Li, Y. Zhang, F. Liu, L. Wang, Z. Wu, Co-Ru alloy nanoparticles decorated onto two-dimensional nitrogen doped carbon nanosheets towards hydrogen/oxygen evolution reaction and oxygen reduction reaction, Journal of Energy Chemistry 87 (2023) 286-294.

https://doi.org/10.1016/j.jechem.2023.08.039.

[22] J. Wang, W. Li, X. Chen, A. Huang, Surface engineering of morphology and electronic structure of CoP by Zn doping for enhanced water splitting performance, Journal of Alloys and Compounds 934 (2023). https://doi.org/10.1016/j.jallcom.2022.167828.

[23] M. Streckova, O. Petrus, A. Guboova, R. Orinakova, V. Girman, C. Bera, M. Batkova, M. Balaz, J. Shepa, J. Dusza, Nanoarchitectonics of binary transition metal phosphides embedded in carbon fibers as a bifunctional electrocatalysts for electrolytic water splitting, Journal of Alloys and Compounds 923 (2022). https://doi.org/10.1016/j.jallcom.2022.166472.

[24] W. Ma, W. Li, H. Zhang, Y. Wang, N-doped carbon wrapped CoFe alloy nanoparticles with MoS_2 nanosheets as electrocatalyst for hydrogen and oxygen evolution reactions, International Journal of Hydrogen Energy 48(58) (2023) 22032-22043. https://doi.org/10.1016/j.ijhydene.2023.03.095.

[25] M. Yue, X. He, S. Sun, Y. Sun, M.S. Hamdy, M. Benaissa, A.A.M. Salih, J. Liu, X. Sun, Co-doped Ni_3S_2 nanosheet array: A high-efficiency electrocatalyst for alkaline seawater oxidation, Nano Research (2023). https://doi.org/10.1007/s12274-023-6002-6.

[26] J. Yang, Y. Wang, J. Yang, Y. Pang, X. Zhu, Y. Lu, Y. Wu, J. Wang, H. Chen, Z. Kou, Z. Shen, Z. Pan, J. Wang, Quench-Induced Surface Engineering Boosts Alkaline Freshwater and Seawater Oxygen Evolution Reaction of Porous $NiCo_2O_4$ Nanowires,

Small 18(3) (2021). https://doi.org/10.1002/smll.202106187.

[27] Y. Song, M. Sun, S. Zhang, X. Zhang, P. Yi, J. Liu, B. Huang, M. Huang, L. Zhang, Alleviating the Work Function of Vein-Like Co_XP by Cr Doping for Enhanced Seawater Electrolysis, Advanced Functional Materials 33(30) (2023). https://doi.org/10.1002/adfm.202214081.

[28] S. Fathima T.K, A. Ghosh, S. Ramaprabhu, ZIF67-derived Co–CoO@C nanocomposites as highly efficient and selective oxygen evolution reaction (OER) catalysts for seawater electrolysis, International Journal of Hydrogen Energy 49 (2024) 780-793. https://doi.org/10.1016/j.ijhydene.2023.09.122.

[29] L. Ji, J. Wang, X. Teng, T.J. Meyer, Z. Chen, CoP Nanoframes as Bifunctional Electrocatalysts for Efficient Overall Water Splitting, ACS Catalysis 10(1) (2019) 412-419. https://doi.org/10.1021/acscatal.9b03623.

[30] L. Huang, D. Chen, G. Luo, Y.R. Lu, C. Chen, Y. Zou, C.L. Dong, Y. Li, S. Wang, Zirconium-Regulation-Induced Bifunctionality in 3D Cobalt-Iron Oxide Nanosheets for Overall Water Splitting, Adv Mater 31(28) (2019) e1901439. https://doi.org/10.1002/adma.201901439.

[31] T. Ouyang, Y.Q. Ye, C.Y. Wu, K. Xiao, Z.Q. Liu, Heterostructures Composed of N-Doped Carbon Nanotubes Encapsulating Cobalt and beta-Mo(2) C Nanoparticles as Bifunctional Electrodes for Water Splitting, Angew Chem Int Ed Engl 58(15) (2019) 4923-4928. https://doi.org/10.1002/anie.201814262.

[32] Y.-Q. Zhang, H.-B. Tao, Z. Chen, M. Li, Y.-F. Sun, B. Hua, J.-L. Luo, In situ

grown cobalt phosphide (CoP) on perovskite nanofibers as an optimized trifunctional electrocatalyst for Zn–air batteries and overall water splitting, Journal of Materials Chemistry A 7(46) (2019) 26607-26617. https://doi.org/10.1039/c9ta08936e.

[33] J. Sun, S. Qin, Z. Zhang, C. Li, X. Xu, Z. Li, X. Meng, Joule heating synthesis of well lattice-matched $Co_2Mo_3O_8/MoO_2$ heterointerfaces with greatly improved hydrogen evolution reaction in alkaline seawater electrolysis with 12.4 % STH efficiency, Applied Catalysis B: Environmental 338 (2023). https://doi.org/10.1016/j.apcatb.2023.123015.

[34] Z. Zhao, J. Sun, Z. Li, X. Xu, Z. Zhang, C. Li, L. Wang, X. Meng, Rapid synthesis of efficient Mo-based electrocatalyst for the hydrogen evolution reaction in alkaline seawater with 11.28% solar-to-hydrogen efficiency, Journal of Materials Chemistry A 11(19) (2023) 10346-10359. https://doi.org/10.1039/d3ta01522j.

[35] Q. Wang, C. Wang, X. Du, X. Zhang, Synthesis of $NiSe_2$@M (M=Cu, Fe and Zn)–NiCo LDH with porous structure on nickel foam for overall fresh and seawater splitting, International Journal of Hydrogen Energy (2023). https://doi.org/10.1016/j.ijhydene.2023.09.133.

[36] S. Gopalakrishnan, V. Saranya, G. Anandha babu, S. Harish, E. Senthil Kumar, M. Navaneethan, Heterogeneous bimetallic oxysulfide nanostructure (Ni-Co) as hybrid bifunctional electrocatalyst for sustainable overall alkaline simulated seawater splitting, Journal of Alloys and Compounds 965 (2023). https://doi.org/10.1016/j.jallcom.2023.171124.

[37] L. Yu, L. Wu, S. Song, B. McElhenny, F. Zhang, S. Chen, Z. Ren, Hydrogen Generation from Seawater Electrolysis over a Sandwich-like NiCoN|Ni_xP|NiCoN Microsheet Array Catalyst, ACS Energy Letters 5(8) (2020) 2681-2689. https://doi.org/10.1021/acsenergylett.0c01244.

[38] L. Wen, X. Li, S. Zhong, P. Zeng, A. Cao, H. Zhang, S.S.A. Shah, X. Hu, W. Cai, Y. Li, Modulating the Electronic Structure of $Co_2P/NiWO_4$ by Interfacial Engineering for Enhanced Seawater Electrolysis, ACS Applied Engineering Materials 1(10) (2023) 2503-2509. https://doi.org/10.1021/acsaenm.3c00338.